

Plastic vortex-creep in $\text{YBa}_2\text{Cu}_3\text{O}_{7-x}$ crystals

Y. Abulafia, A. Shaulov, Y. Wolfus, R. Prozorov, L. Burlachkov, and Y. Yeshurun

*Institute of Superconductivity, Department of Physics,
Bar-Ilan University, Ramat-Gan 52900, Israel*

D. Majer and E. Zeldov

*Department of Condensed Matter Physics, The Weizmann Institute of Science,
Rehovot 76100, Israel*

H. Wühl

*Forschungszentrum Karlsruhe, Institut für Technische Physik and
Universität Karlsruhe, D-76021 Karlsruhe, Germany*

V.B. Geshkenbein

*Theoretische Physik, ETH Zürich-Hönggerberg, CH-8093 Zürich,
Switzerland and L.D. Landau Institute for Theoretical Physics, 117940
Moscow, Russia*

V.M. Vinokur

Argonne National Laboratory, Argonne, IL 60439, USA

Abstract

Local magnetic relaxation measurements in $\text{YBa}_2\text{Cu}_3\text{O}_{7-x}$ crystals show evidence for plastic vortex-creep associated with the motion of dislocations in the vortex lattice. This creep mechanism governs the vortex dynamics in a wide range of temperatures and fields below the melting line and above the field corresponding to the peak in the "fishtail" magnetization. In this range the

activation energy U_{pl} , which decreases with field, drops below the elastic (collective) creep activation energy, U_{el} , which increases with field. A crossover in flux dynamics from elastic to plastic creep is shown to be the origin of the fishtail in $\text{YBa}_2\text{Cu}_3\text{O}_{7-x}$.

PACS numbers: 74.60.Ge, 74.72.Bk

Magnetic relaxation in high-temperature superconductors has been traditionally described in terms of collective vortex-creep based on the concept of elastic motion of the vortex lattice [1,2]. This approach successfully explained wide range of vortex dynamics phenomena. On the other hand, under certain conditions effects of vortex lattice *plasticity* may become the dominant factor that determines the vortex dynamics [3]. For example, numerical simulations of strongly pinned vortex system reveal vortex motion dominated by plastic deformations [4]. Experimentally, effects of plastic vortex behavior were observed in transport measurements in close vicinity of the melting transition where the pre-melting softening of the lattice enhances the role of spatial inhomogeneities, resulting in the tearing of the vortex lattice under applied currents [5,6]. In this paper we demonstrate that plastic deformations dominate vortex-lattice motion in the creep regime in $\text{YBa}_2\text{Cu}_3\text{O}_{7-x}$ (YBCO) crystals far below the melting transition, in the region that was believed to be governed by elastic motion. We find that this plastic motion governs the flux creep in YBCO crystals at elevated temperatures at fields above the characteristic field B_p corresponding to the peak in the 'fishtail' magnetization [7–14], and it affects the corresponding shape of the magnetization curves.

The plastic vortex motion can be classified into three main categories. i) Vortex channeling along easy paths in the pinning relief in between rather stationary vortex-lattice islands. Such behavior was observed in numerical simulations in presence of very strong pinning [4]. ii) Vortex motion that resembles ice floe in which large pieces of vortex-lattice slide with respect to each other. As was simulated numerically [15], these two modes of dynamics are believed to be the cause of the highly unstable character of resistivity in the close vicinity of the melting transition [5,6]. iii) Dislocation mediated plastic creep of vortex lattice similar

to diffusion of dislocations in atomic solids [16]. This type of vortex behavior was considered previously [17,18] without an experimental evidence. The observations described below strongly suggest that this mode of plastic vortex creep governs magnetic relaxation over a substantial part of the YBCO magnetic phase diagram.

Local magnetic relaxation measurements were performed on a $1.2 \times 0.5 \times 0.3 \text{ mm}^3$ single crystal of YBCO ($T_c \simeq 91 \text{ K}$) using an array of microscopic GaAs/AlGaAs Hall sensors with $30 \times 30 \text{ }\mu\text{m}^2$ active area and sensitivity better than 0.1 G . The probes detect the component B_z of the field normal to the surface of the crystal. Temperature stability and resolution was better than 0.01 K .

After zero-field-cooling (*zfc*) the sample from above T_c to the measurement temperature T we measured the full hysteresis loops for all the probes. The first field for full penetration H^* was measured directly by the probe at the center of the sample. After repeating the *zfc* process, a *dc* field H was applied parallel to the *c*-axis and the local induction B_z was measured at different locations as a function of the time t for an hour. These relaxation measurements were repeated after the field was increased by a step $\Delta H > 2H^*$ up to the irreversibility field H_{irr} or the maximum field of the experiment (1.6 T).

The inset to Figure 1 shows typical hysteresis loops, $B_z^{(i)} - H$ vs. H at $T = 85 \text{ K}$ for four probes ($i = 5, 6, 7, 8$ located at 70, 130, 190, and $250 \text{ }\mu\text{m}$ from the edge towards the center). Each probe exhibits a clear fishtail behavior with a maximum in local magnetization at field $B_p \simeq 0.4 \text{ T}$. The width of the loop is largest in the center of the crystal and decreases towards the edges, as expected from basic considerations based on a modified Bean model [19].

In Figure 1 we show the time evolution of the gradient $(B_z^{(6)} - B_z^{(7)})/\Delta x$ between $t_1 = 8 \text{ sec}$ and $t_2 = 3600 \text{ sec}$, as a function of the applied field. In our geometry (aspect ratio $= 3/5$) this gradient is proportional to the persistent current density J that can be readily evaluated using sensors 6 and 7 which are located not too close to the center or the edge of the crystal [20–22]. Note that the position of the fishtail peak B_p shifts from 0.42 T to 0.34 T during the relaxation. The total relaxation of the current, ΔJ , during the time

window of the measurement is large for $B < B_p$ and it increases to even larger values above B_p . Furthermore, the relative change of the persistent current, $\Delta J/J$, is also large (e.g. $\Delta J/J \approx 0.8$ at $H = 0.9 T$), implying that $J \ll J_c$ on both sides of the fishtail peak. These strong relaxations imply that dynamic effects determine the shape of $J(B)$ and rule out the possibility [7,8,12] that either branch of the fishtail is determined by the critical current density $J_c(B)$.

Knowledge of the time and spatial field-derivatives, $\partial B_z/\partial t$ and $\partial B_z/\partial x$, enable direct determination [22] of the activation energy $U(J, B)$ associated with the flux creep by using the diffusion equation: $\partial B_z/\partial t = -\partial/\partial x(B_z v)$, where the effective vortex velocity v is proportional to $\exp(-U/kT)$. Typical U vs. J data, at 85 K, are shown in Fig. 2 for different fields, in the range of 0.05 T to 0.8 T. This figure exhibits a dramatic crossover in the slope $|dU/dJ|$ around $B_p = 0.4 T$. In order to quantify this crossover, we start by using the prediction of the collective creep theory for $J \ll J_c$ [1,17]:

$$U(B, J) = U_0(B)(J_c/J)^\mu \propto B^\nu J^{-\mu}, \quad (1)$$

where the positive critical exponents ν and μ depend on the specific pinning regime. We note that the range of the experimentally accessible U -values in Fig. 2 is almost independent of the field [23]. This implies $J \propto B^{\nu/\mu}$, i.e. J grows with field for $J \ll J_c$. Obviously, the collective creep dynamics cannot explain the decrease of J with B observed above B_p .

The inset to Fig. 2 shows the μ -values obtained by fitting the $U(J)$ data, using Eq. 1. At low fields $\mu \simeq 1$ and it then increases to $\mu \simeq 2$ just below B_p . This confirms [8] that below the peak the relaxation is well described by the collective creep theory. The latter predicts $\mu = 1$ in the intermediate bundle regime and $\mu = 5/2$ in the small bundle regime [24]. However, above the peak, μ drops sharply to values below 0.2. Within the collective creep theory this would imply an inconceivable crossover to a single vortex regime ($\mu = 1/7$) which is expected only for low fields and high values of J [1]. Thus the μ -values above B_p are inconsistent with the collective creep theory.

The failure of the collective creep theory in explaining the data above B_p can be further

demonstrated by analyzing the exponent ν in Eq. (1). Separation of variables in this equation implies that a smooth $U(J)$ function can be obtained by proper field-scaling of the data sets at various fields. However, as demonstrated in Fig. 3 we need *two* exponents of *opposite signs*, $\nu \cong 0.7$ and $\nu \cong -1.2$, to scale the data of Fig. 2 for fields below and above B_p , respectively. In the collective creep theory U increases with B , thus the *negative* ν -value is inconsistent with this theory.

We now show that the experimental data above B_p can be well explained by a plastic creep model based on dislocation mediated motion of vortices similar to diffusion of dislocations in atomic solids [16]. The activation energy U_{pl}^0 at $J = 0$ for the motion of a dislocation in the vortex lattice can be estimated as [18]:

$$U_{pl}^0(B) \simeq \varepsilon \varepsilon_0 a \propto 1/\sqrt{B} \quad (2)$$

where ε_0 is the vortex line tension, $\varepsilon = \sqrt{m_{ab}/m_c}$ is the anisotropy parameter, and $a \simeq \sqrt{\phi_0/B}$ is the mean intervortex distance. This estimation assumes a formation of a dislocation semi-loop between two valleys separated by a distance a [16]. One notices that U_{pl}^0 *decreases* with field in contrast to the collective creep activation energies U_{el} , which *increases* with field, see Eq. (1). Of course, the creep process is governed by the smaller between U_{el} and U_{pl} . Thus, at low fields where $U_{pl} > U_{el}$, the latter controls the flux dynamics. But, as B increases and U_{pl} becomes less than U_{el} , a crossover to the plastic creep regime is expected.

The values of $U_{pl}^0(B)$ can be extracted from the measured $U(J)$ curves of Fig. 2 assuming an expression for $U_{pl}(J)$ taken from the dislocation theory [16], substituting the current density for the strain:

$$U_{pl}(J) = U_{pl}^0 \left(1 - \sqrt{J/J_c^{pl}} \right), \quad (3)$$

where J_c^{pl} is the critical current which corresponds to the plastic motion. The derived U_{pl}^0 values are shown in the inset of Fig. 3 as a function of B . The solid line in the inset is a power-law fit to the experimental data, $U_{pl}^0 \propto B^{-0.7}$. Clearly, U_{pl}^0 decreases with the field,

although with an exponent -0.7 rather than the expected -0.5 . As we show below, the same exponent (-0.7) is also involved in determining the temperature dependence of B_p .

The fishtail peak location B_p can be determined from the condition $U_{el} = U_{pl}$ for the same J . Note that $U_{pl} \cong U_{pl}^0$ since $J \ll J_c^{pl}$. Using the logarithmic solution of the flux diffusion equation [1] $U_{el} = kT \ln(t/t_0)$ together with Eq. (2), we get $B_p \propto 1/\ln^2(t/t_0)$, i.e. the peak position should shift with time towards low fields, as observed in Fig. 1. Similarly, for the temperature dependence of B_p one obtains:

$$B_p \propto \varepsilon_0^2 \propto 1/\lambda^4 \propto \left(1 - (T/T_c)^4\right)^2. \quad (4)$$

A fit of this expression to the experimental data yields a modest agreement. However, as noted above, in fact $U_{pl}^0 \propto B^{-0.7}$, thus $B_p(T) \propto \varepsilon_0^{1/0.7}$, i.e. $B_p \propto (1 - (T/T_c)^4)^{1.4}$. Indeed, a perfect fit (B_p , solid line in Fig. 4) is obtained with this expression. Note that a similar variation of the exponent was found in some experiments [25] for the melting line $B_m(T) \propto (1 - (T/T_c))^1$, while the theory [1] predicted a critical exponent of 2. This interesting similarity may support previous claims [6] that the plastic motion of defects in the vortex lattice is a precursor to the melting transition.

In Figure 4 we show that the plastic creep regime in the $B - T$ phase diagram (shaded area) covers a substantial area between the $B_p(T)$ line found in this experiment and the melting line $B_m(T)$ described in Ref. [25].

In conclusion, our data clearly indicate two different flux-creep mechanisms above and below the peak in the magnetization curves. In particular, flux creep with activation energy *decreasing* with field plays an important role above the peak. The data in this regime cannot be explained in terms of the traditional collective creep theory based on the concept of elastic motion of the vortex lattice. On the other hand, the data show good agreement with the dislocation mediated mechanism of plastic creep analogous to plasticity in atomic solids. This observation leads also to the conclusion that the origin of the fishtail in YBCO crystals is a crossover from elastic to plastic creep. The predictions of this model for the time and temperature dependence of the location of the peak are well confirmed in the experiments.

We thank H. Shtrikman for growing the GaAs heterostructures, and acknowledge useful discussions with M. Konczykowski and P. Kes. This work was supported in part by the Israel Academy of Science and Humanities, the Heinrich Hertz Minerva Center for High Temperature Superconductivity, and the DG XII, Commission of the European Communities, administered by the Israeli Ministry of Science and the Arts. Y.Y. and E.Z. acknowledge support of the U.S.A.-Israel Binational Science Foundation. A.S. and E. Z. acknowledge support from the France-Israel cooperation program AFIRST. V.B.G. is grateful to ITP at UCSB for the support via grant PHY94-07194. V.M.V. acknowledges support from the US Department of Energy, BES - Material Sciences, under contract no. W-31-109-ENG-38. The visits of V.B.G. and V.M.V. to Bar-Ilan were supported by the Rich Foundation.

REFERENCES

- [1] G. Blatter, M.V. Feigel'man, V.B. Geshkenbein, A.I. Larkin, and V.M. Vinokur, Rev. Mod. Phys. **66**, 1125 (1994).
- [2] E.H. Brandt, Reports on Progress in Physics, 1996, to be published.
- [3] M.V. Feigel'man, V.B. Geshkenbein, and A.I. Larkin, Physica C **167**, 177 (1990); V.M. Vinokur, P.H. Kes, and A.E. Koshelev, Physica C **168**, 29 (1990); C.J. van der Beek and P.H. Kes, Phys. Rev. B **43**, 13032 (1991).
- [4] H.J. Jensen, A. Brass, A.-C. Shi, and A.J. Berlinsky, Phys. Rev. B **41**, 6394 (1990); A.E. Koshelev and V.M. Vinokur, Phys. Rev. Lett. **73**, 3580 (1994).
- [5] S. Bhattacharya and M.J. Higgins, Phys. Rev. B **49**, 10005 (1994); H. Safar *et al.*, Phys. Rev. B **52**, 6211 (1995).
- [6] W.K. Kwok, J.A. Fendrich, C.J. van der Beek, and G.W. Crabtree, Phys. Rev. Lett. **73**, 2614 (1994).
- [7] M. Daeumling, J.M. Seutjens, and D.C. Larbalestier, Nature (London) **346**, 332 (1990).
- [8] L. Krusin-Elbaum, L. Civale, V.M. Vinokur, and F. Holtzberg, Phys. Rev. Lett. **69**, 2280 (1992).
- [9] S.N. Gordeev, W. Jahn, A.A. Zhukov, H. Küpfer, and T. Wolf, Phys. Rev. B **49**, 15420 (1994).
- [10] Y. Yeshurun *et al.*, Proc. of the 7th International Workshop on "Critical Currents in Superconductors", Alpbach, Austria, 1994, p. 237.
- [11] L. Klein, E.R. Yacoby, Y. Yeshurun, A. Erb, G. Muller-Vogt, V. Breit and H. Wuhl Phys. Rev. B **49**, 4403 (1994).
- [12] H. Küpfer, S.N. Gordeev, W. Jahn, R. Kresse, R. Meier-Hirmer, T. Wolf, A.A. Zhukov, K. Salama and D. Lee, Phys. Rev. B **50**, 7016 (1994).

- [13] A.A. Zhukov, H. K  pfer, G. Perkins, L.F. Cohen, A.D. Caplin, S.A. Klestov, H. Claus, V.I. Voronkova, T. Wolf, and H. W  hl, Phys. Rev. B **51**, 12704 (1995).
- [14] Hai-hu Wen, H.G. Schnack, R. Griessen, B. Dam, and J. Rector, Physica C **241**, 353 (1995).
- [15] D.W. Braun *et al.*, Phys. Rev. Lett. **76**, 831 (1996); I. Aranson and V.M. Vinokur, unpublished.
- [16] J.P. Hirth and J. Lothe, *Theory of Dislocations*, Ch. 15, John Wiley & Sons, NY, 1982.
- [17] M.V. Feigel'man, V.B. Geshkenbein, A.I. Larkin, and V.M. Vinokur, Phys. Rev. Lett. **63**, 2303 (1989).
- [18] V.B. Geshkenbein, A.I. Larkin, M.V. Feigel'man, and M.V. Vinokur, Physica C **162-164**, 239 (1989).
- [19] R. Prozorov *et al.*, J. Appl. Phys. **76**, 7621 (1995).
- [20] Y. Abulafia *et al.*, "Coherence in High- T_c Superconductors", Eds. A. Revolevski and G. Deutscher, World Science Publishing (Singapore), 1996.
- [21] H. Brandt and M. Indenbom, Phys. Rev. B **48**, 12893 (1993); E. Zeldov, J.R. Clem, M. McElfresh, and M. Darwin, Phys. Rev. B **49**, 9802 (1994).
- [22] Y. Abulafia, A. Shaulov, Y. Wolfus, R. Prozorov, L. Burlachkov, Y. Yeshurun, D. Majer, E. Zeldov, and V.M. Vinokur, Phys. Rev. Lett. **75**, 2404 (1995).
- [23] This is consistent with the logarithmic solution of the flux diffusion equation [1] $U(t) = kT \ln(t/t_0)$ for the fixed experimental time window $t_1 < t < t_2$, since the only field dependent parameter in $U(t)$ is the time scale t_0 under the logarithm.
- [24] The intermediate bundle regime ($\mu \approx 1$) corresponds to lower fields where the characteristic energy $U_0(B)$ is small, and thus for a constant U , the ratio J_c/J is large, see Eq. 1. This implies that J relaxes down deeply below J_c , thus reaching this regime, see

[1]. As the field increases $U_0(B)$ increases thus J_c/J decreases and J enters the small bundle regime with $\mu \approx 5/2$.

[25] H. Safar, P.L. Gammel, D.A. Huse, D.J. Bishop, W.C. Lee, and D.M. Ginsberg, Phys. Rev. Lett. **70**, 3800 (1993); R. Liang, D. A. Bonn, and W. N. Hardy, Phys. Rev. Lett. **76**, 835 (1996).

FIGURE CAPTIONS

Fig. 1 Relaxation of persistent current J calculated from the field gradients for different applied fields at $T = 85\text{ K}$. Note the shift in the peak position B_p during the experimental time window 8 – 3600 sec as noted by the arrows. Also note the increase in the relaxation rate above B_p . Inset: Local hysteresis loops for four Hall probes vs. applied field H at $T = 85\text{ K}$. The width of the loops increases from the edge of the sample towards the center.

Fig. 2 U vs. J for the indicated fields ($0.05\text{ T} - 0.8\text{ T}$) at $T = 85\text{ K}$. The lines are guide to the eye. Note the change in the slope $\partial U/\partial j$ above and below the peak field $B_p \simeq 0.4\text{ T}$. Inset: The critical exponent μ , see Eq. (1), as a function of field, at $T = 85\text{ K}$.

Fig. 3 Scaling of $U(J, B)$ -curves below and above B_p at $T = 85\text{ K}$. Above the peak $U \propto B^{0.7}$ and below the peak $U \propto B^{-1.2}$. The inset shows the derived U_{pl}^0 vs. B . The solid line is a fit to $U_{pl} \propto B^{-0.7}$.

Fig. 4 Vortex-creep phase diagram for YBCO. The plastic creep regime is limited between $B_p(T)$ (solid line) and the melting line $B_m(T)$ (dashed line, taken from [25]). Data points in the $B_p(T)$ curve were determined in this experiment at $t_1 = 8\text{ sec}$. The solid line is a fit to $B_p \propto (1 - (T/T_c)^4)^{1.4}$.

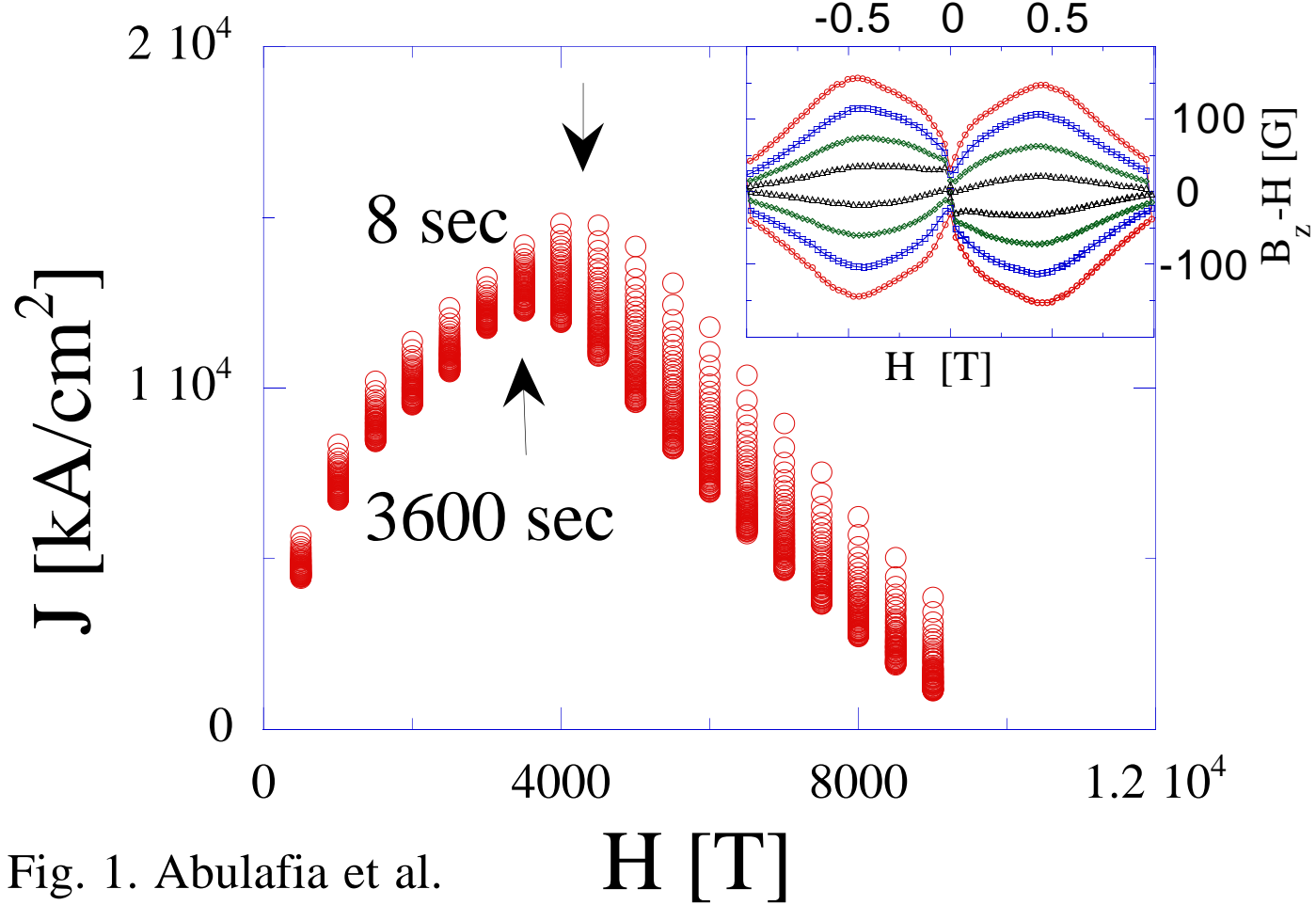


Fig. 1. Abulafia et al.

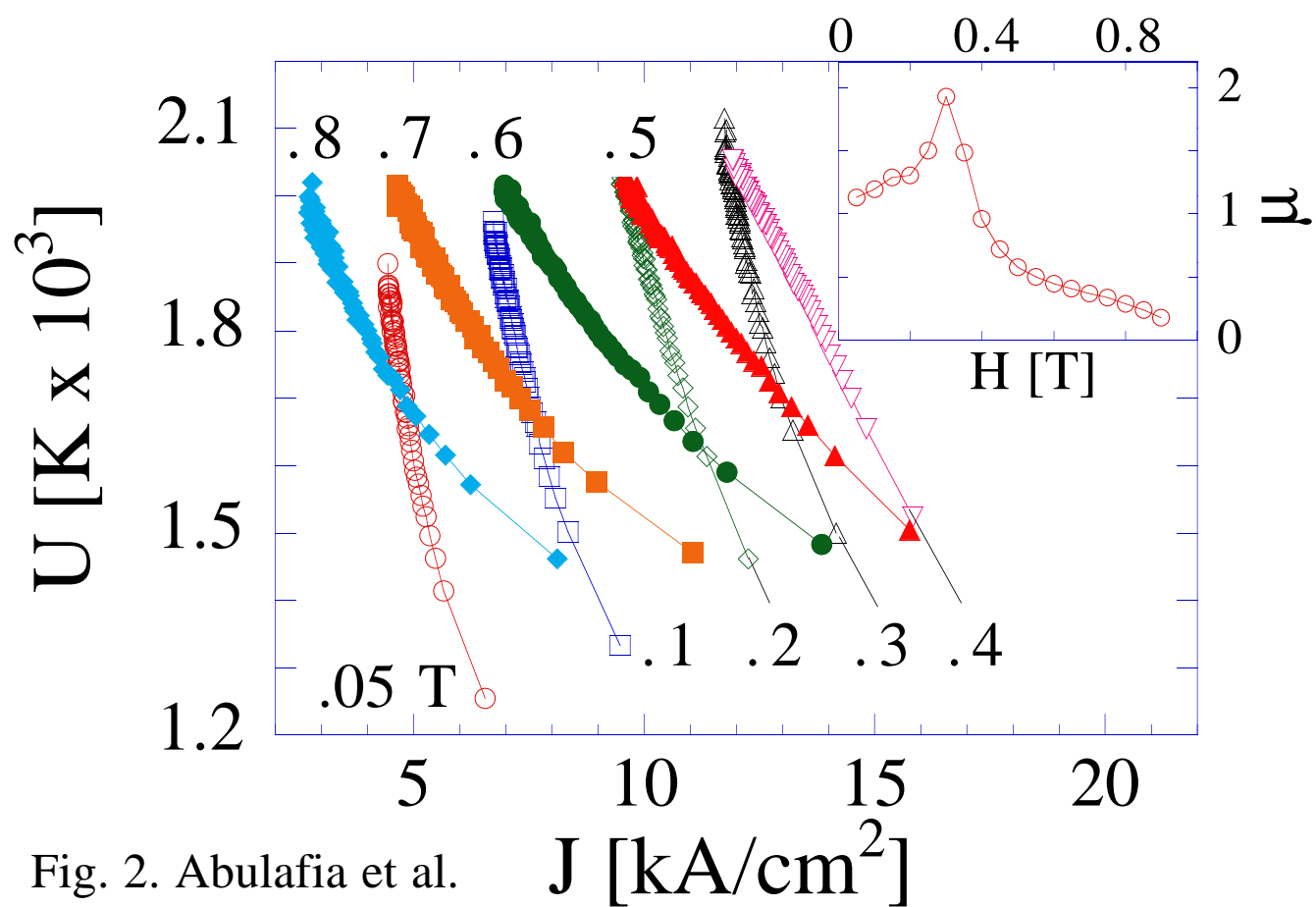


Fig. 2. Abulafia et al.

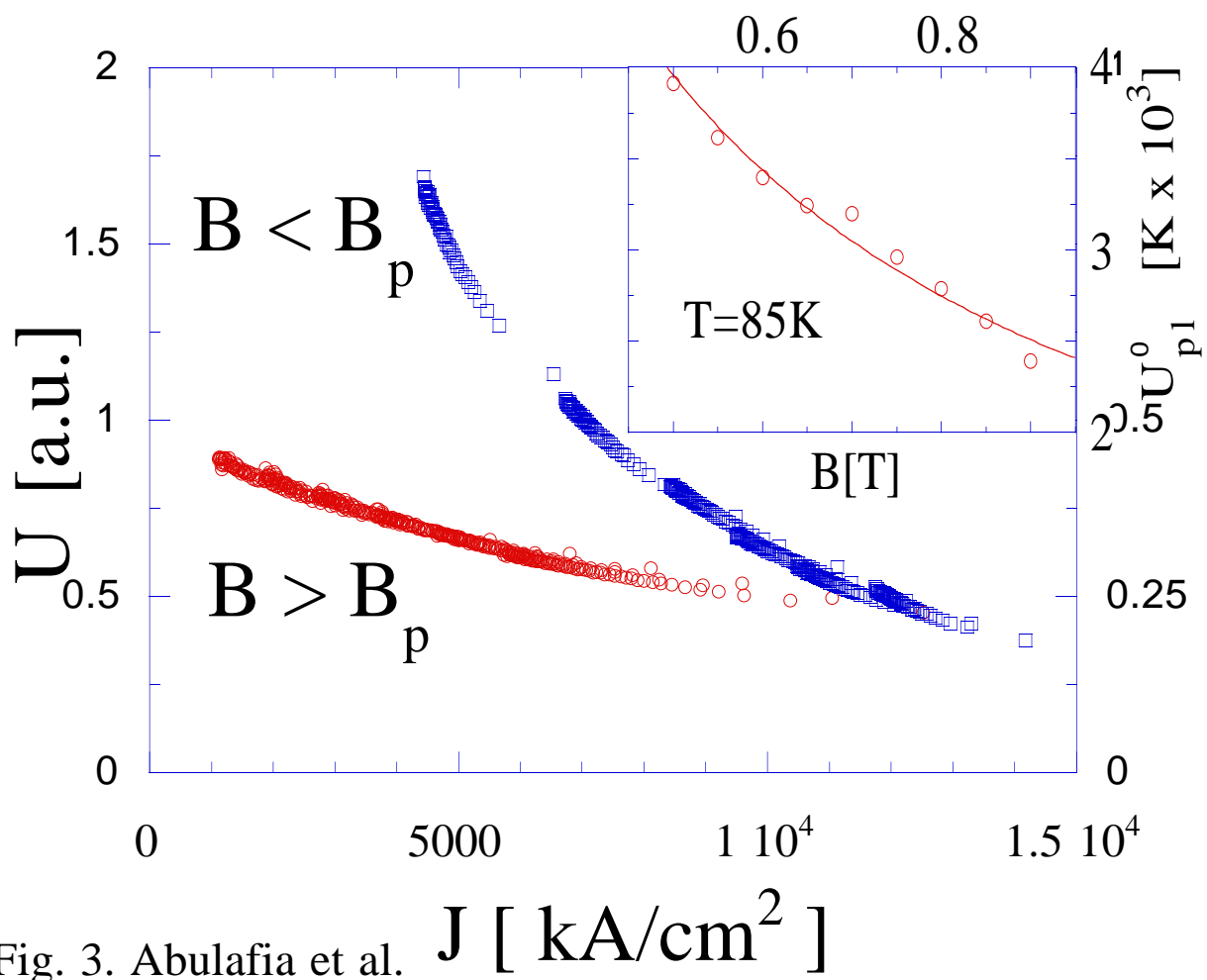


Fig. 3. Abulafia et al. J [kA/cm²]

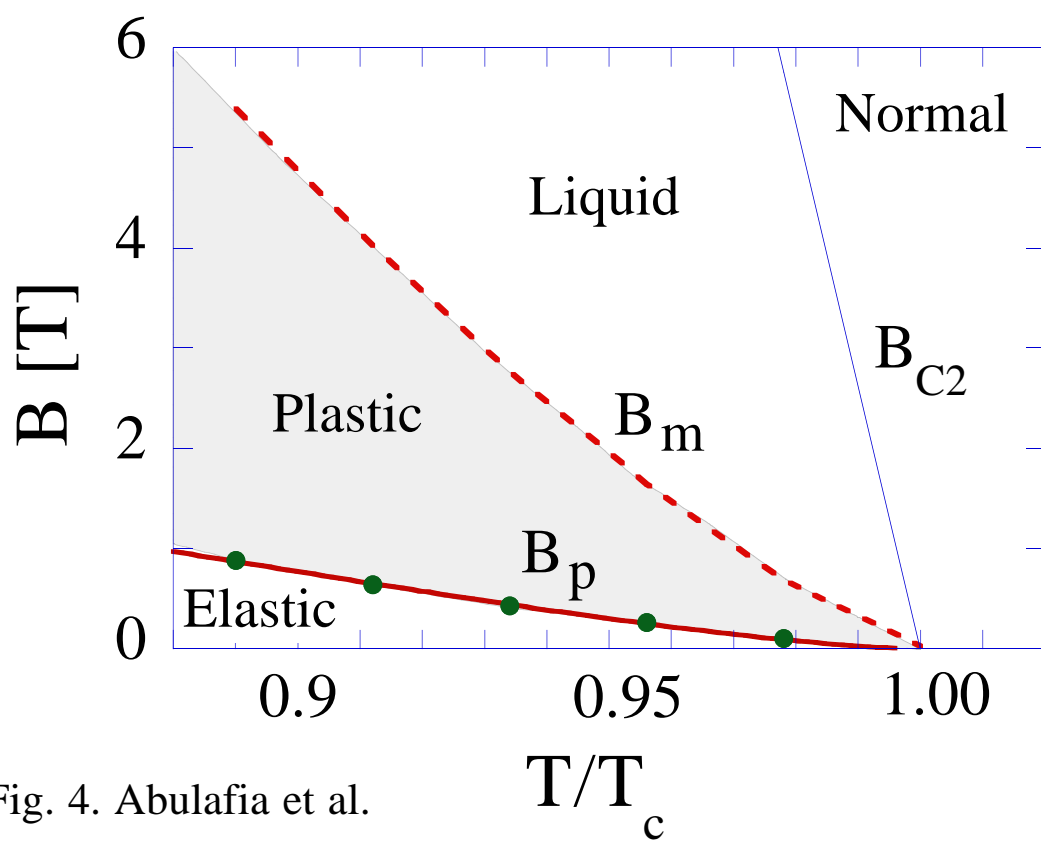


Fig. 4. Abulafia et al.